Document Title: Correction of Fresnel reflection of the sky dome accounting for the polarisation

Version: 1.0

Author(s): R. Santer and F. Zagolski

Affiliation(s): ADRINORD, Association pour le Développement de la Recherche et de l'Innovation dans la Région Nord-Pas de Calais, Lille – France.

Executive summary

The ocean colour from satellite measurements is characterized by the water reflectance. In situ measurements of the water reflectance are performed in our 2Seas region to validate the satellite products.

A field radiometer measures the water leaving radiance which has two sources: (i) The signal from the ocean which is the useful component. (ii) The reflection of the atmospheric radiance which has to be subtracted

A second radiometer measured the atmospheric radiance. The standard correction is based on applying the Fresnel coefficient for the view angle. This approach ignored the polarisation both of the atmospheric scattering and of the Fresnel reflection. This report after a sensitivity study, aims defining a new protocol to better correct from the sky dome reflection. This new protocol will be applied to the in situ data base collected in the 2Seas region.

List of tables and figures

Figure 2: Fresnel coefficient R1 (left) and degree of polarisation (100R2/R1). By convention, P<0 corresponds to a direction of vibration perpendicular to the scattering plane.

Figure 3: scattering angle versus solar zenith angle in the TRIOS MUMM and Seaprism geometries

Figure 4: Phase function versus solar zenith angle: Rayleigh (double light cross), M1 (blue diamond), M2 (red square), M3 (green triangle), M4 (cross)

Figure 5: Polarization ratio versus solar zenith angle: Rayleigh (double light cross), M1 (blue diamond), M2 (red square), M3 (green triangle), M4 (cross)

Figure 6: Polarization ratio versus solar zenith angle: Rayleigh (blue diamond), M1 with an AOT at 550 nm of 0.3 (red square), 0.6 (green triangle) and 0.9 (blue cross). Upper plot at 412 nm, lower plot at 753 nm.

Figure 7: Polarization ratio versus solar zenith angle: Rayleigh (blue diamond), M2 with an AOT at 550 nm of 0.3 (red square), 0.6 (green triangle) and 0.9 (blue cross). Upper plot at 412 nm, lower plot at 753 nm.

Figure 8: Polarization ratio versus solar zenith angle: Rayleigh (blue diamond), M3 with an AOT at 550 nm of 0.3 (red square), 0.6 (green triangle) and 0.9 (blue cross). Upper plot at 412 nm, lower plot at 753 nm

Figure 9: Polarization ratio versus solar zenith angle: Rayleigh (blue diamond), M1 with an AOT at 550 nm of 0.3 (red square), 0.6 (green triangle) and 0.9 (blue cross). Upper plot at 412 nm, lower plot at 753 nm.

Figure 10: Specular. Absolute bias on the water reflectance versus solar zenith angle: Rayleigh (blue diamond), M1 with an AOT at 550 nm of 0.3 (red square), 0.6 (green triangle) and 0.9 (blue cross). Left plot at 412 nm, right plot at 753 nm.

Figure 11: Specular. Absolute bias on the water reflectance versus solar zenith angle: Rayleigh (blue diamond), M2 with an AOT at 550 nm of 0.3 (red square), 0.6 (green triangle) and 0.9 (blue cross). Left plot at 412 nm, right plot at 753 nm.

Figure 12: Specular. Absolute bias on the water reflectance versus solar zenith angle: Rayleigh (blue diamond), M3 with an AOT at 550 nm of 0.3 (red square), 0.6 (green triangle) and 0.9 (blue cross). Left plot at 412 nm, right plot at 753 nm.

Figure 13: Specular. Absolute bias on the water reflectance versus solar zenith angle: Rayleigh (blue diamond), M4 with an AOT at 550 nm of 0.3 (red square), 0.6 (green triangle) and 0.9 (blue cross). Upper plot at 412 nm, lower plot at 753 nm.

Figure 14: Specular. Absolute bias on the water reflectance for two solar zenith angles versus the wavelength: Rayleigh (blue diamond), M4 with an AOT at 550 nm of 0.3 (red square), 0.6 (green triangle) and 0.9 (blue cross)

Figure 15: Reflection coefficient at 520 nm versus the solar zenith angle. The aerosol model is the model 3. Rayleigh (blue diamond), M4 with an AOT at 550 nm of 0.3 (red square), 0.6 (green triangle) and 0.9 (blue cross)

Figure 16: M3 with AOT=0.3 at 550 nm: Spectral dependence of the reflection coefficient at 2 SZA for three wind speeds: 1 m/s (blue diamond), 5 m/s (red square) and 10 m/s (green triangle)

Figure 17: Wind speed of 1 m/s. Absolute bias on the water reflectance for two solar zenith angles versus the wavelength: The AOT at 550 nm is for M1 (blue diamond), M2 (red square), M3 (blue cross) and 0.9 (green triangle).

List of acronyms

ADRINORD	Association pour le Developpement de la Recherche et de l'Innovation dand le NORD
AOT	Aerosol Optical Thickness
BOA	Bottom Of Atmosphere
MERIS	Medium Resolution Imaging Spectrometer (ESA Envisat)
MUMM	Management Unit of the North Sea Mathematical Models
SAA	Solar Azimuth Angle
SOS	Sucessive orders of scattering
SZA	Solar Azimuth Angle
TOA	Top Of Atmosphere
VAA	View Azimuth Angle
VZA	View Zenith Angle

1) Introduction

1.1) Generality

We are in the frame of the validation of the atmospheric correction through the characterization of the optical properties of the water surface.

The level 1 corresponds to monochromatic TOA radiances at the nominal wavelength of each spectral band. As a first approximation, the gaseous transmittance is a multiplicative factor which is corrected upstream.

Equation (1) introduces the contribution of the atmospheric path radiance and of the water leaving radiance;

$$L_{toa}(\lambda,\theta_s,\theta_v,\Delta\varphi) = L_{atm}(\lambda,\theta_s,\theta_v,\Delta\varphi) + T(\theta_v)\ L_w(\lambda,\theta_s,\theta_v,\Delta\varphi) \quad (1)$$

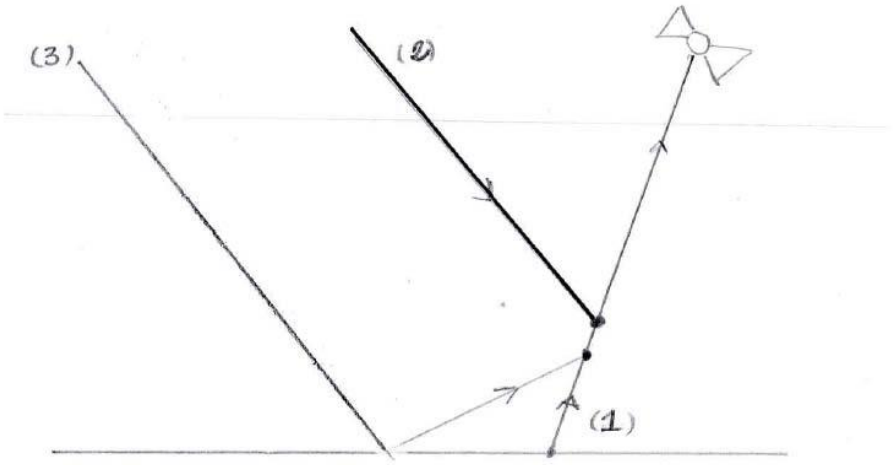

Figure 1: schematic decomposition of the TOA signal

At TOA, the direction of the sun $\vec{s}_0$ is defined by the solar zenith angle (SZA), ϑ_s , and the solar azimuth angle (SAA), φ_s . The viewing direction $\vec{s}$ is referred by the view zenith angle (VZA), ϑ_v and the view azimuth angle (VAA), φ_v .

In equation (1), the direct sunglint is negligible or has been perfectly corrected. There is no correction by the foam.

The water leaving radiance is weighted by the total transmittance defined, using the principle of reciprocity, as the ratio between the surface atmospheric irradiance normalized by the TOA irradiance.

The water leaving radiance is weighted by the total transmittance defined, using the principle of reciprocity, as the ratio between the surface atmospheric irradiance normalized by the TOA irradiance.

Atmospheric irradiance is the sum of the direct and of the diffuse computed over a dark surface.

$$T(\theta) = \exp(-\tau / \mu) + t_d(\theta) \tag{2}$$

Actually, we should consider, equation (3), the water leaving radiance observed on the direct to direct path L_w from the water radiance in the vicinity $< L_w >$ which is scattered toward the sensor.

$$L_{toa} = L_{atm} + L_w \exp(-\tau / \mu_v) + < L_w > t_d(\theta_v) \tag{3}$$

The ratio of the direct to the diffuse is reported in table 1. Clearly, we cannot neglect the contribution of the adjacent pixels except in case of a perfect spatial homogeneity of the ocean optical properties or if an accurate correction of the adjacency effect has been done. If so, we are back to equation (1). If not, we can go back to equation (1) assuming that the adjacency effects are corrected.

AOT/VZA(°)	6.5	28.8	73.3
0.000	88.3	86.7	61.9
0.244	70.4	70.4	29.3
0.449	58.1	54.2	15.3
0.859	39.5	35.1	4.1

Table 1: Direct to total transmittance ratio at 412 nm in percent for 3 VZA and for different AOT.

In order to conduct the atmospheric correction, the first step is to know the molecular scattering through the knowledge of the barometric pressure and the second step is to define the aerosol model which is from case 1 conducted for example in the NIR over the back ocean for case 1 water.

By normalization of the radiance by the TOA incident solar irradiance, we get the 5S formalism:

$$\rho_{toa} = \rho_{atm} + T(\theta_s)\rho_w T(\theta_v) \tag{4}$$

The down-welling transmittance $T(\theta_s)$ is the ratio of the BOA irradiance to the TOA irradiance.

$L_w^{\uparrow}$ can be converted as well in above water reflectance (or water remote sensing reflectance by ignoring π) as follows:

$$\rho_w^{\uparrow} = \frac{\pi \cdot L_w^{\uparrow}}{E_0^{\downarrow}(\vartheta_s)} = \frac{\pi \cdot L_w^{\uparrow}}{\mu_s E_s T(\vartheta_s)} \tag{5}$$

which is the parameter employed in the MERIS data processing.

At the end, equation (1) remains the fundamental equation. Thanks to break points in the L2 processor, we have all the atmospheric functions to play with equations (5) and (4) to go back to equation (3).

On a radiometric point of view, the key message is that the validation of the atmospheric correction should be conducted on $L_w^{\uparrow}$ and not on ρ_w. The two parameters $L_w^{\uparrow}$ and ρ_w are comparable only if we are under clear sky condition, allowing having:

$$T(\theta_s) = E_0^+ / (\mu_s E_s) \tag{6}$$

With the possibility to relate the theoretical estimation of $T(\theta_s)$ with the measurement of E_0^+.

On a geophysical point of view, when once wants to interpret the colour of the water, we also need to validate equation (6) if we use equation (4) to get ρ_w.

In this report, we just focus on $L_w^{\uparrow}$. Having in mind that L_{atm} contains the coupling between atmospheric scattering and Fresnel reflection, we first have to remove the sky dome reflection from the measurement of the radiance above water. We also have to remove the direct sunglint L_G^0. For MERIS, the reflectance of the sunglint ρ_G is computed using the Cox and Muk wave slope distribution associated to the wind speed. At a given wavelength, the direct attenuation of the solar beam is computed with the Rayleigh optical thickness and the aerosol optical thickness computed from the MERIS aerosol product.

1.2) The standard correction of the sky dome reflection

Downward $L^{\downarrow}(\vartheta_s, \vartheta_v, \varphi_s - \varphi_v)$ and upward $L^{\uparrow}(\vartheta_s, \vartheta_v, \varphi_s - \varphi_v)$ are acquired with the same VAA but with two opposite VZAs.

If the sea is perfectly flat, the water leaving radiance $L_w^{\uparrow}$ is expressed as:

$$L_w^{\uparrow} = L^{\uparrow} - R(\vartheta_v) \cdot L^{\downarrow} \tag{7}$$

where $R(\vartheta_v)$ is the Fresnel reflection coefficient.

They are sophisticated formulations of equation (6). The roughness of the sea surface invites to refine this formulation corresponding to a flat sea surface with:

$$L_w^{\uparrow} = L^{\uparrow} - R(\vartheta_v, w) \cdot L^{\downarrow} - L_G(w) \exp(-\tau / \mu_s) \tag{8}$$

In equation (8) first appears a Fresnel reflection coefficient which depends on the wind speed, the driving parameter for the roughness of the sea surface.

Second, even if the geometrical conditions are selected to avoid as much as possible the direct sunglint, we can subtract this residue. To be consistent with the MERIS processor, we use the Cox and Munk wave slope distribution model associated to the wind speed. The attenuation on the direct solar path is computed knowing the Rayleigh and aerosol optical thicknesses. The first is computed from the barometric pressure, For the second, different options are possible: in situ measurement of the optical thickness, computation for satellite matchup using the L2 aerosol product, interpretation of $L^{\downarrow}$.

Some authors also subtract the water leaving radiance observed in the NIR (750 nm):

$$L_w^{\uparrow}(\lambda) = L_w^{\uparrow}(\lambda) - L_w^{\uparrow}(750nm) \tag{9}$$

based on the darkness of the water body. This “white” correction can potentially include the contribution of the foam. It is may be relevant where the foam contribution is corrected on the satellite imagery which is not the case for MERIS.

1.3) Introduction of the polarisation on the reflection of the sky dome

The equation (7) does not account for the polarisation of the radiance field. When the VZA is enough large, the Fresnel reflection becomes polarized. In the blue, the sky radiance is also polarized and these two combined effects bias equation (7) which is based on a scalar approach of the radiative transfer.

The downwelling radiance is described by the Stokes parameters (I,Q,U,V). Actually, both for the Rayleigh and the Mie scatterings, we can neglect the ellepticity V. According to the Snellius-Fresnel laws, the reflection coefficients of the amplitude of the incident electric field in the parallel (rl) and the perpendicular (rp) directions to the incidence plane are written as:

$$rl = -[\tan(i-r)]/[\tan(i+r)] \quad (10)$$

$$rr = -[\sin(i-r)]/[\sin(i+r)] \quad (11)$$

with, i the incident angle and r the refracted angle. Using the Descartes law (refractive index of air being equal to 1.34

$$\sin(i) = nw \,.\, \sin(r) \quad (12)$$

The reflection matrix (R) on the water surface is:

$$R = \begin{bmatrix} R1 & R2 & 0 \\ R2 & R1 & 0 \\ 0 & 0 & R3 \end{bmatrix} \quad (13)$$

With:

$$R1 = (1/2).[(rl)^2+(rr)^2]$$

$$R2 = (1/2).[(rl)^2-(rr)^2] \quad (14)$$

$$R3 = rl.rr$$

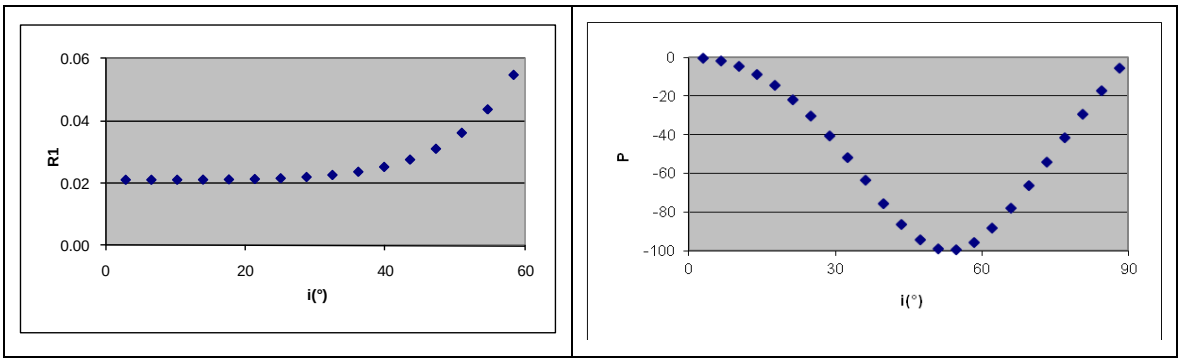

Figure 2: Fresnel coefficient R1 (left) and degree of polarisation (100R2/R1). By convention, P<0 corresponds to a direction of vibration perpendicular to the scattering plane.

2) The SOS computations

2.1) The tests cases

Tool: SOS code in polarisation (Deuzé et al)

Inputs:

Solar value=

0°+ 20 Gaussian as SZA, the MUMM view geometry: SVA=40°, phi=135°.

MERIS bands 1 to 10

Cox and Munk associated to three wind speeds: 1, 5 and 10 m/s. No direct sun glint.

Black ocean body

4 aerosol models (M1, M2, M3, and M4): power law associated to Angstroem coefficient values of -0.4, -1, -1.5, -2 with a refractive index of 1.44.

Four AOT at 550 nm: 0 (Rayleigh), 0.3, 0.6 and 0.9

Outputs:

Sky radiance at surface (Stokes parameters: I, Q, U, V is negligible)) and reflected radiance in the MUMM geometry (VZA=40°, f=135°)

Total down welling radiance

Some remarks:

(i) The last value of the SZA is 70°. MERIS acquired a little further up to 75°, but the atmospheric correction performances are not expected to be accurate enough. The default option in MERMAID is to exclude SZA above 60°.

(ii) The view geometry corresponds to the MUMM TRIOS values. It is always possible to duplicate this study thanks to the simulator. For the Seaprism, the geometry differs with f=90°. At a given VZA, the driven geometrical parameter is the scattering angle Θ given by:

$$\cos(\Theta) = \mu_s \mu_v + \sin(\theta_s)\sin(\theta_v)\cos(\varphi) \quad (15)$$

Figure 3 gives the correspondence between the scattering angle and the VZA. For the TRIOS, we reach the maximum of polarisation of the Rayleigh around $\Theta = 90°$. The Seaprism does not go so far, but the residual contamination by the sunglint should be higher as well as the sky radiance because the forward scattering is more effective.

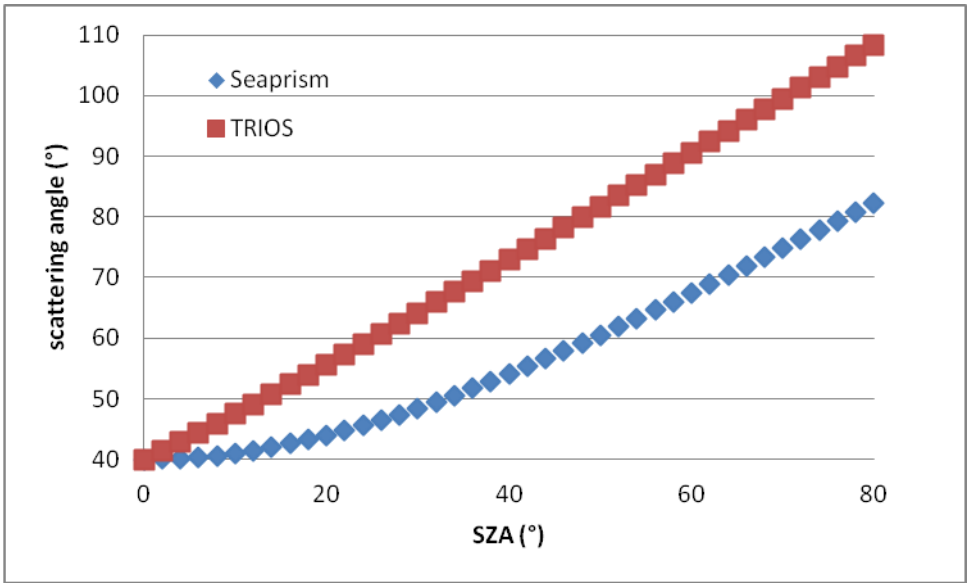

Figure 3: scattering angle versus solar zenith angle in the TRIOS MUMM and Seaprism geometries

(iii) We stop the analysis in band 10 at 751 nm. It covers the domain of the ocean colour. For the NIR, those bands are available in the simulator. But because the Rayleigh, the major source of polarisation, strongly decreases in the NIR, we do not expect to see a major influence of the polarisation in the NIR.

(iv) The Cox and Munk model is selected for consistency with MERIS. For the TRIOS, we follow the present protocol which is to not correct from the direct sunglint.

(v) The ocean body is black, it results that we ignore the coupling between the quasi Lambertian reflection of the ocean and the atmospheric scattering. First, it is consistent with the MERIS formalism for which this coupling is neglected in the computation of the total transmittance for the downward path. Second, this coupling is non polarised simply because a lambertian reflection does not generate polarisation. Actually in the formalism used for the atmospheric correction, the ocean body and the atmosphere are characterized by their albedo: the water reflectance and the atmospheric spherical albedo.

(vi) We use power laws simply because they optical properties do not vary with wavelength and this helps for the analysis.

(vii) We first compute for the Rayleigh, AOT=0.3 is a mean value for the coastal zones in which most of the in situ data are collected. AOT=0.6 is the turbid case. AOT=0.9 corresponds to the limit of the performance of the atmospheric correction algorithm.

(viii) We output the Stokes parameters for the sky radiance, instead of simply the radiance because it will be useful to compute the specular reflection.

(ix) We output the total transmittance in order to convert a radiance into a reflectance. .

2.2 Analyze the data base

Figure 4 gives the phase functions for the Rayleigh and the 4 aerosol models. Figure 5 gives the polarization ratio P (the ratio between the two first terms of the phase matrix: In the domain SZA=(30°-60)° the sky radiance can be strongly polarised. The negative value of P indicates that the maximum of polarised light is perpendicular to the principal plane.

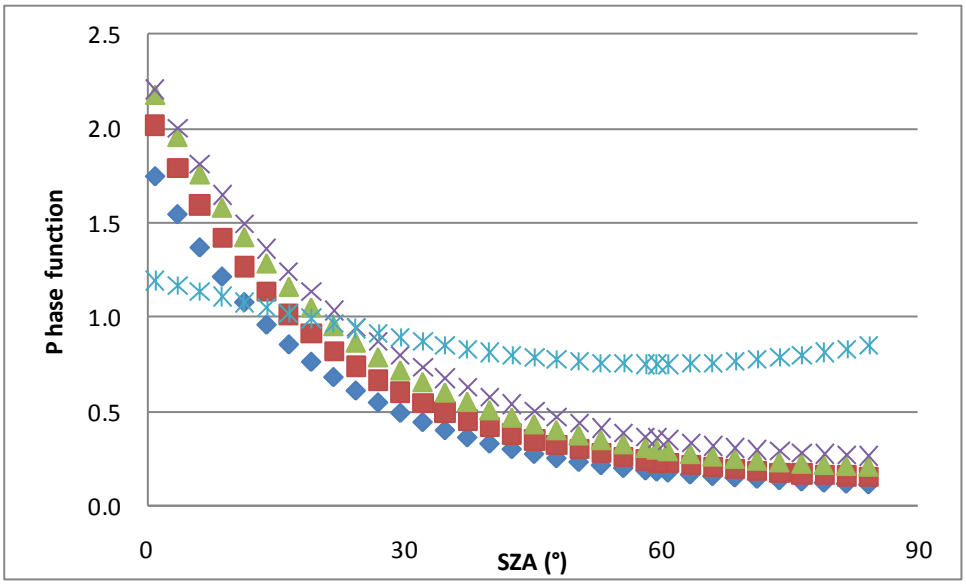

Figure 4: Phase function versus solar zenith angle: Rayleigh (double light cross), M1 (blue diamond), M2 (red square), M3 (green triangle), M4 (cross)

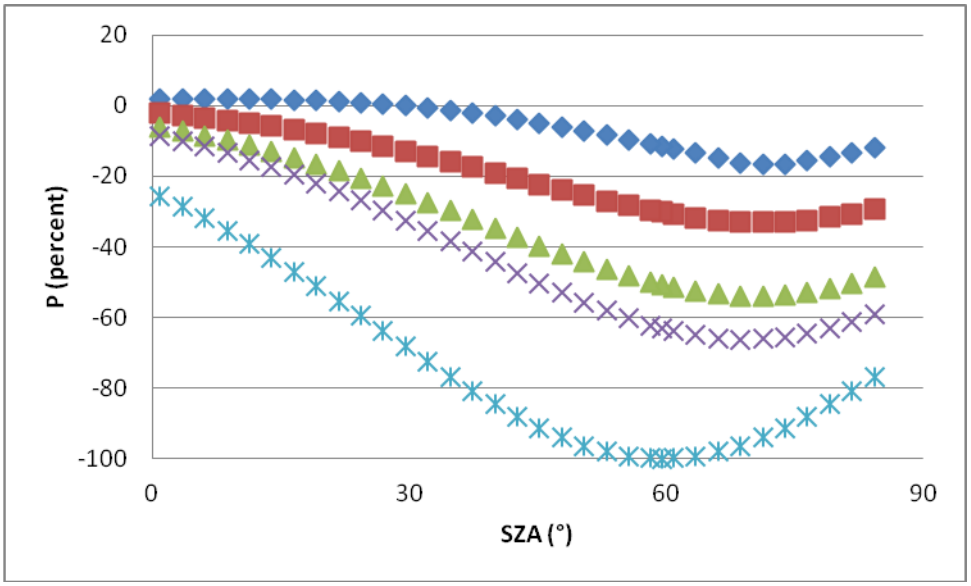

Figure 5: Polarization ratio versus solar zenith angle: Rayleigh (double light cross), M1 (blue diamond), M2 (red square), M3 (green triangle), M4 (cross)

The multiple scattering modifies the polarisation. The polarisation ratio $P = 100\frac{\sqrt{(Q^2+U^2}}{I}$ is reported figures 6 to 9. Also notice that, because of the definition P is now positive.

Well known characteristics appear:

(i) Multiple scattering depolarizes. The Rayleigh is less polarized in the blue than in the red.

(ii) The presence of aerosols depolarizes the Rayleigh more effectively with large aerosols which polarised less.

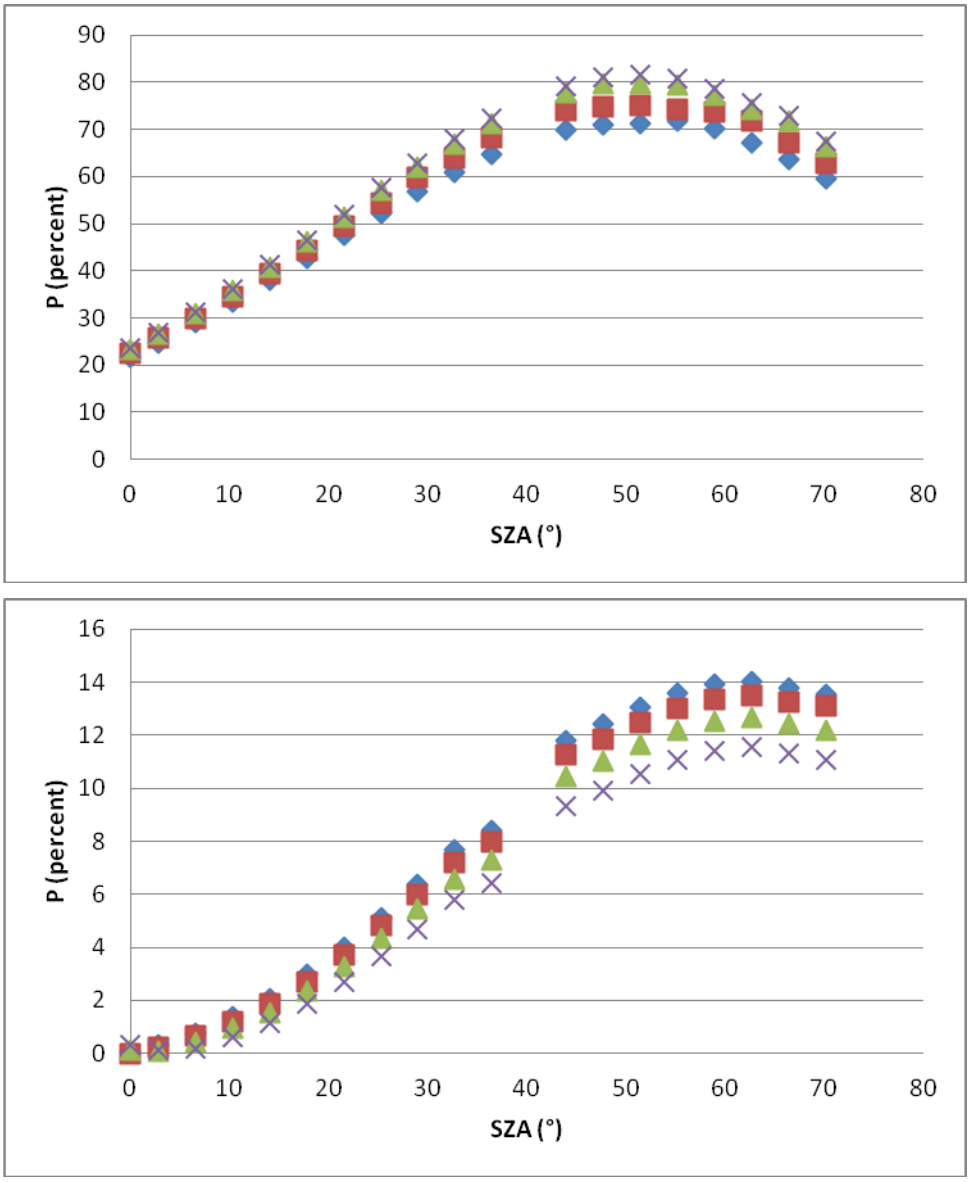

Figure 6: Polarization ratio versus solar zenith angle: Rayleigh (blue diamond), M1 with an AOT at 550 nm of 0.3 (red square), 0.6 (green triangle) and 0.9 (blue cross). Upper plot at 412 nm, lower plot at 753 nm.

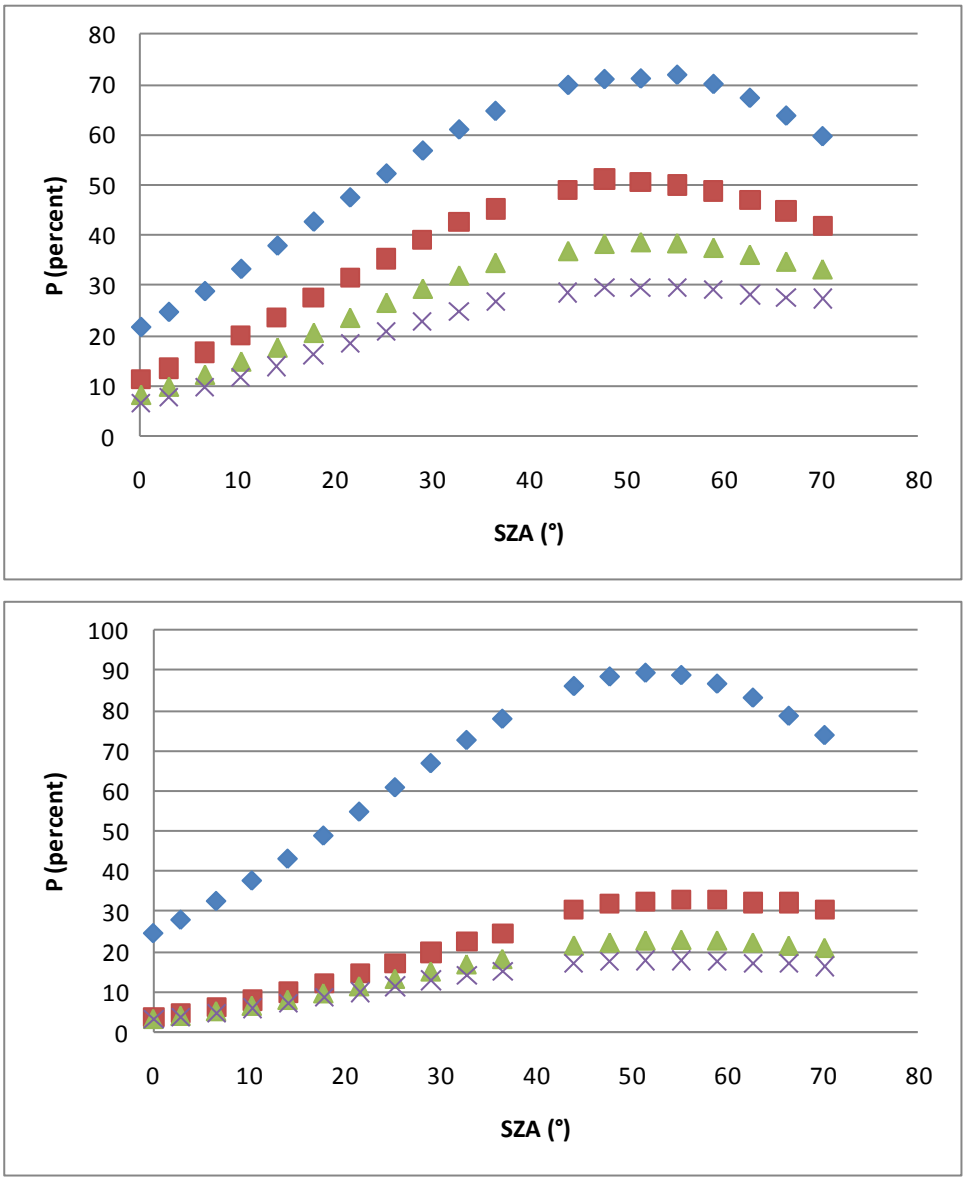

Figure 7: Polarization ratio versus solar zenith angle: Rayleigh (blue diamond), M2 with an AOT at 550 nm of 0.3 (red square), 0.6 (green triangle) and 0.9 (blue cross). Upper plot at 412 nm, lower plot at 753 nm.

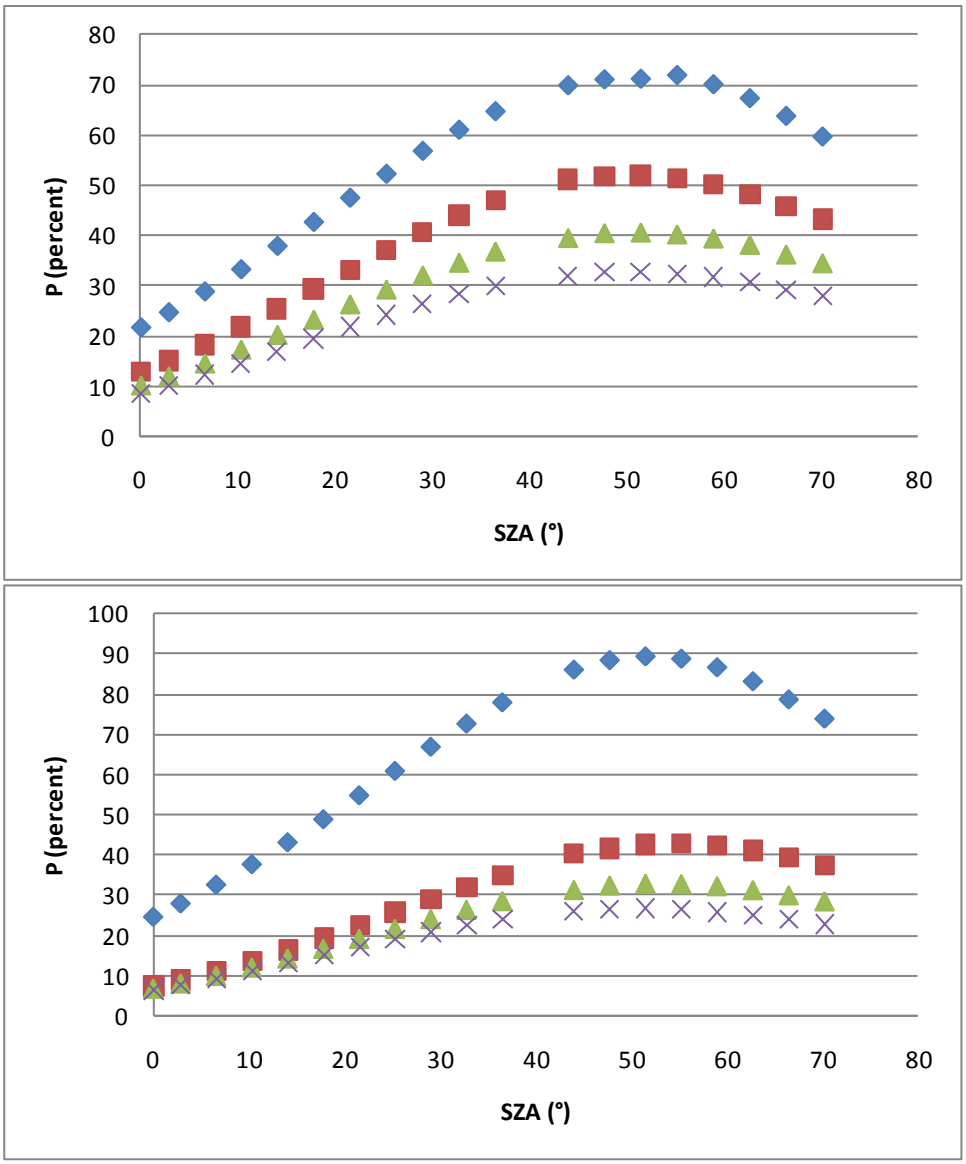

Figure 8: Polarization ratio versus solar zenith angle: Rayleigh (blue diamond), M3 with an AOT at 550 nm of 0.3 (red square), 0.6 (green triangle) and 0.9 (blue cross). Upper plot at 412 nm, lower plot at 753 nm.

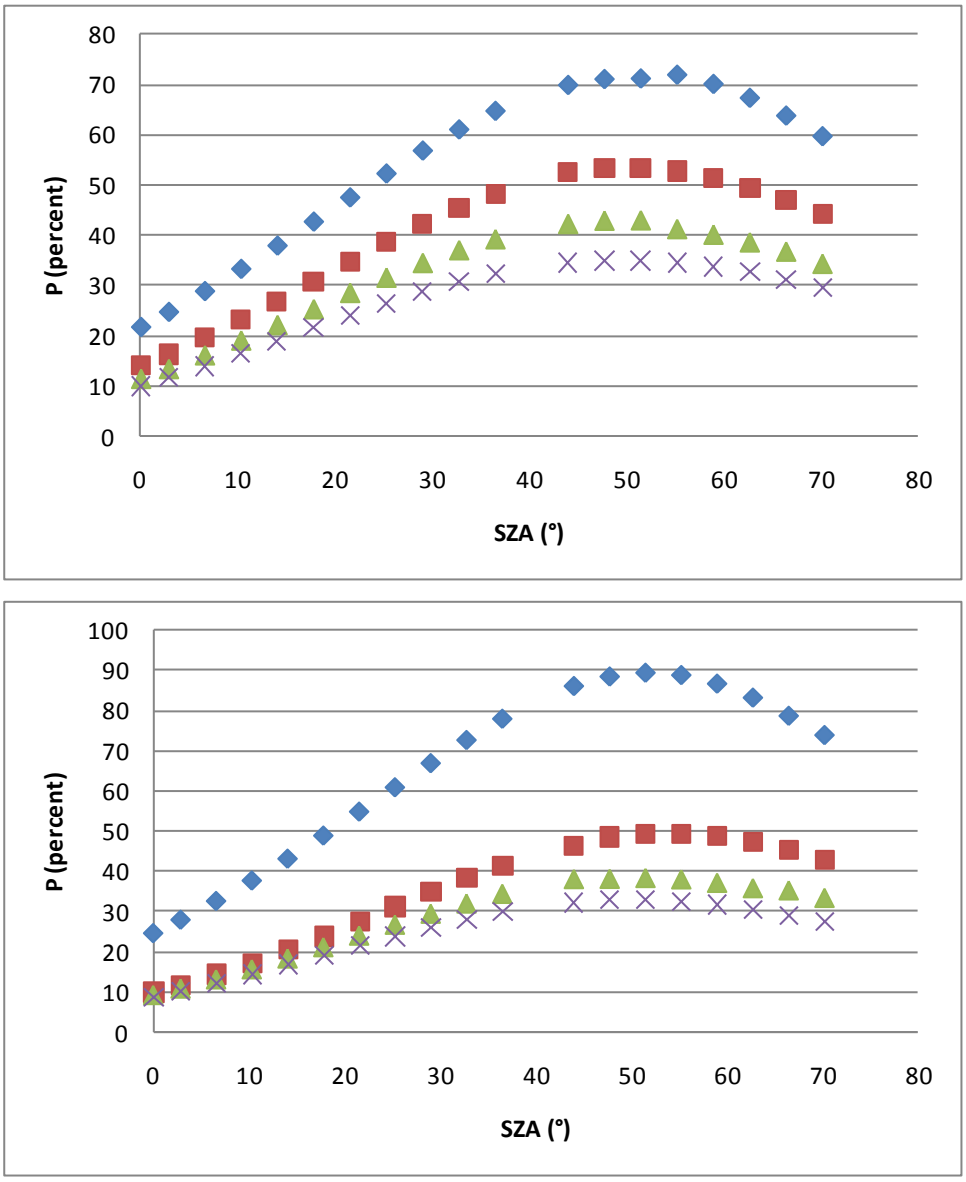

Figure 9: Polarization ratio versus solar zenith angle: Rayleigh (blue diamond), M1 with an AOT at 550 nm of 0.3 (red square), 0.6 (green triangle) and 0.9 (blue cross). Upper plot at 412 nm, lower plot at 753 nm.

3 Influence of the polarisation on the sky dome reflection

3.1 The specular reflection

Basis equations

We indicated above the properties of the Fresnel reflection. The down-welling radiance is characterized by the Stokes parameters (I,Q,U,V). V is negligible. After multiplication by the Fresnel matrix, the reflection of the sky dome is:

$$I^{\uparrow} = R_1 I^{\downarrow} + R_2 Q^{\downarrow} + R_3 U^{\downarrow} \tag{16}$$

The Rayleigh is totally polarised at a scattering angle of 90°. In figure 3 this scattering angle appears at SZA=62°.

For SZA=62° both the Rayleigh scattering and the Fresnel reflection are strongly polarized and:

$$I^{\uparrow} = 2R_1 I^{\downarrow} \tag{17}$$

It this case there is using equation (7) a missing factor 2 on the correction.

The radiance reflected by a horizontal surface is:

The scalar case: $I_{up}=I_{down}*R_1$

The polar case: $I_{up}=I_{down}*R_1 +Q_{down}*R_2+ U_{down}*R_3$

For a water refractive index of 1.33, the values (*100) of the Fresnel coefficient for a VZA=40° are:

R1	R2	R3
2.527	-1.907	1.658

Table 2: Fresnel reflection coefficients at an incident angle of 40°

The standard protocol ignores the polarization. The error on the correction in radiance is

$$dI_{up}=Q_{down}*R_2+ U_{down}*R_3 \tag{18}$$

The error on the water reflectance, derived from equation (5) is:

$$d\rho_w = \frac{dI_{up}}{\mu_s T(\vartheta_s)} \tag{19}$$

The errors are given in absolute values on the water reflectance expresses in percent. These errors on the water reflectance are reported for the four aerosol models in figures 10 to 13. At 440 nm, the error is not strongly dependent on the aerosols, both type and abundance. The Rayleigh polarization is the main source. The error increases with the SZA. For two reasons:

(i) the polarisation is going to it maximum at SZA at 62°.

(ii) the total transmittance decreases with the SZA which increases in proportion $d\rho_w$

Having in mind, standard values of the water reflectance of few percent, neglecting the polarisation has a major impact.

In the red, first the errors are much more smaller because of the vanishing contribution of the Rayleigh. A consequence, is that we can see the impact of the polarisation.of the aerosol scattering which is more effective with small aerosols (see M4)..

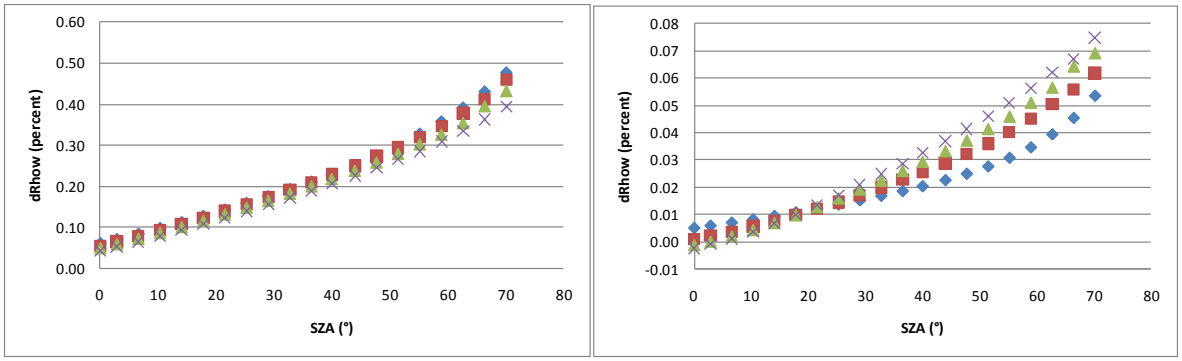

Figure 10: Specular. Absolute bias on the water reflectance versus solar zenith angle: Rayleigh (blue diamond), M1 with an AOT at 550 nm of 0.3 (red square), 0.6 (green triangle) and 0.9 (blue cross). Left plot at 412 nm, right plot at 753 nm.

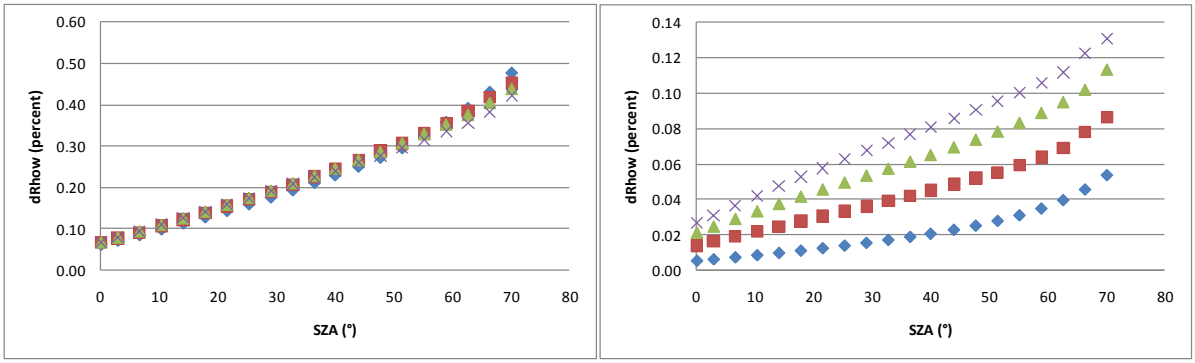

Figure 11: Same as figure 10 but for M2

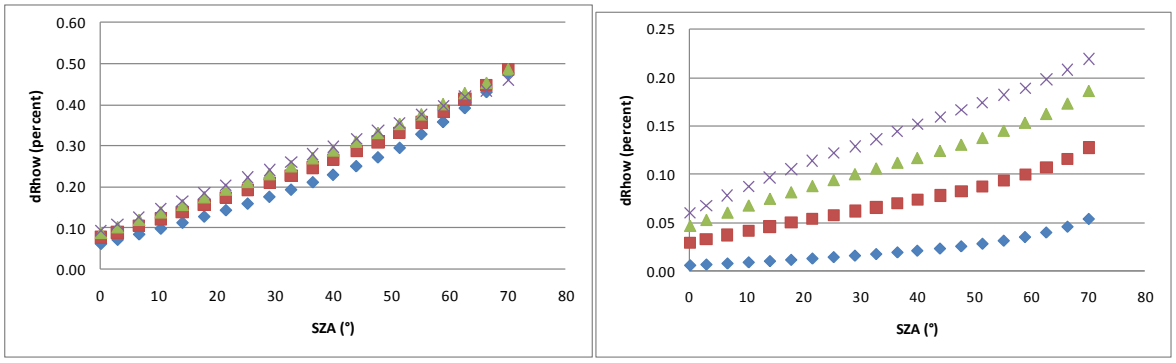

Figure 12: Same as figure 10 but for M3

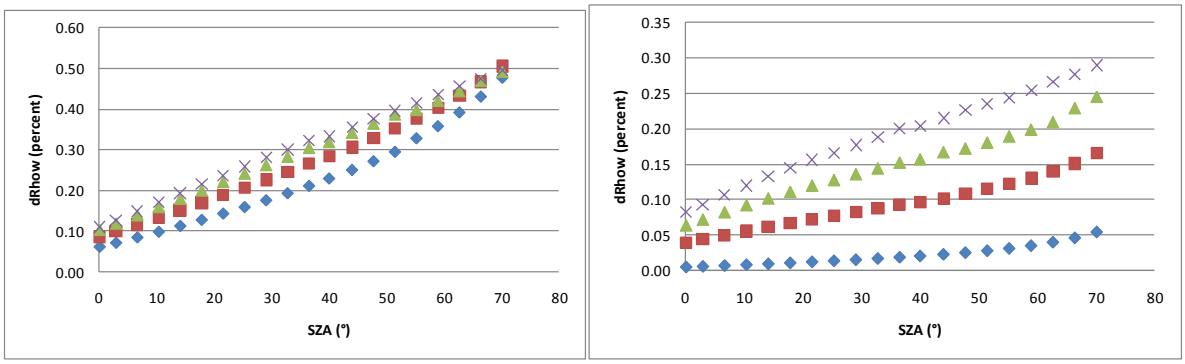

Figure 13: Same as figure 10 but for M4.

The figure 14 gives the spectral dependence of the error for M4 to see the extreme impact of the aerosols.

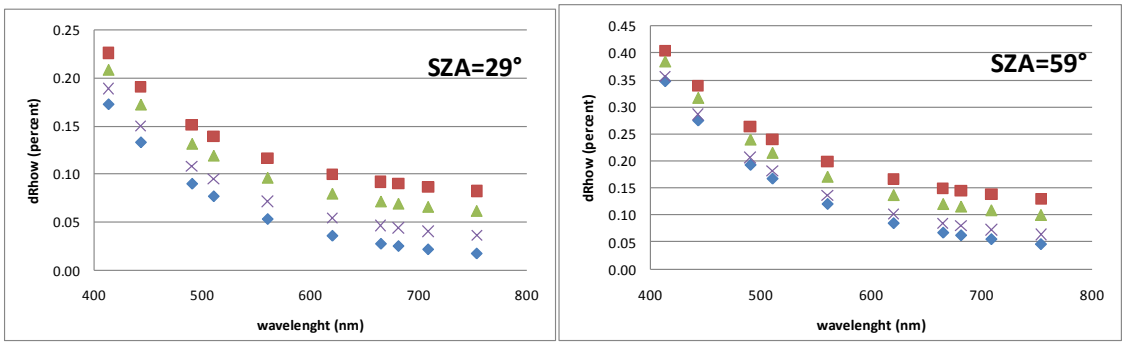

Figure 14: Specular. Absolute bias on the water reflectance for two solar zenith angles versus the wavelength: Rayleigh (blue diamond), M4 with an AOT at 550 nm of 0.3 (blue cros), 0.6 (green triangle) and 0.9 (red square) Left plot at 412 nm, right plot at 753 nm.

3.2) Influence of the wind speed on the reflection of the sky dome

We first compute the reflection coefficient R (percent) following Eq. (24) Ruddick et al, 2006 for the 3 wind s peed values:

w(m/s)	1	5	10
R	2.560	2.84	3.29

Table 3: Reflection coefficients as provided by Ruddick et al, 2006.

These values correspond to a clear sky; under cloudy condition, the isotropy of the sky radiance makes the roughness of the ocean a secondary parameter. The isotropic condition also removes the polarization. Therefore, a simple recommendation in this case is to keep the reflection coefficient of 0.256 proposed by Ruddick et al, 2006.

From the SO code computations, the coefficient of reflection R_{SOS} is the ratio on the radiance at surface between upwelling and down welling. For a given wavelength and M3, figure 15, R does not depends much on the AOT as soon as we are not in the Rayleigh regime.

Figure 15 gives the influence of the wind speed at 510 nm. We are always above the values of table 3, which means that the standard correction under evaluates the reflection. Clearly, our R:

(i) Depends on the SZA.

(ii) Depends on the atmospheric conditions.

(iii) is higher because of the polarization.

At high wind speeds (10 m/s), we also see at low SZA, the influence of the sunglint. R also slightly decreases with the AOT. The multiple scattering regimes depolarizes: the intensity increases more rapidly than the polarized component.

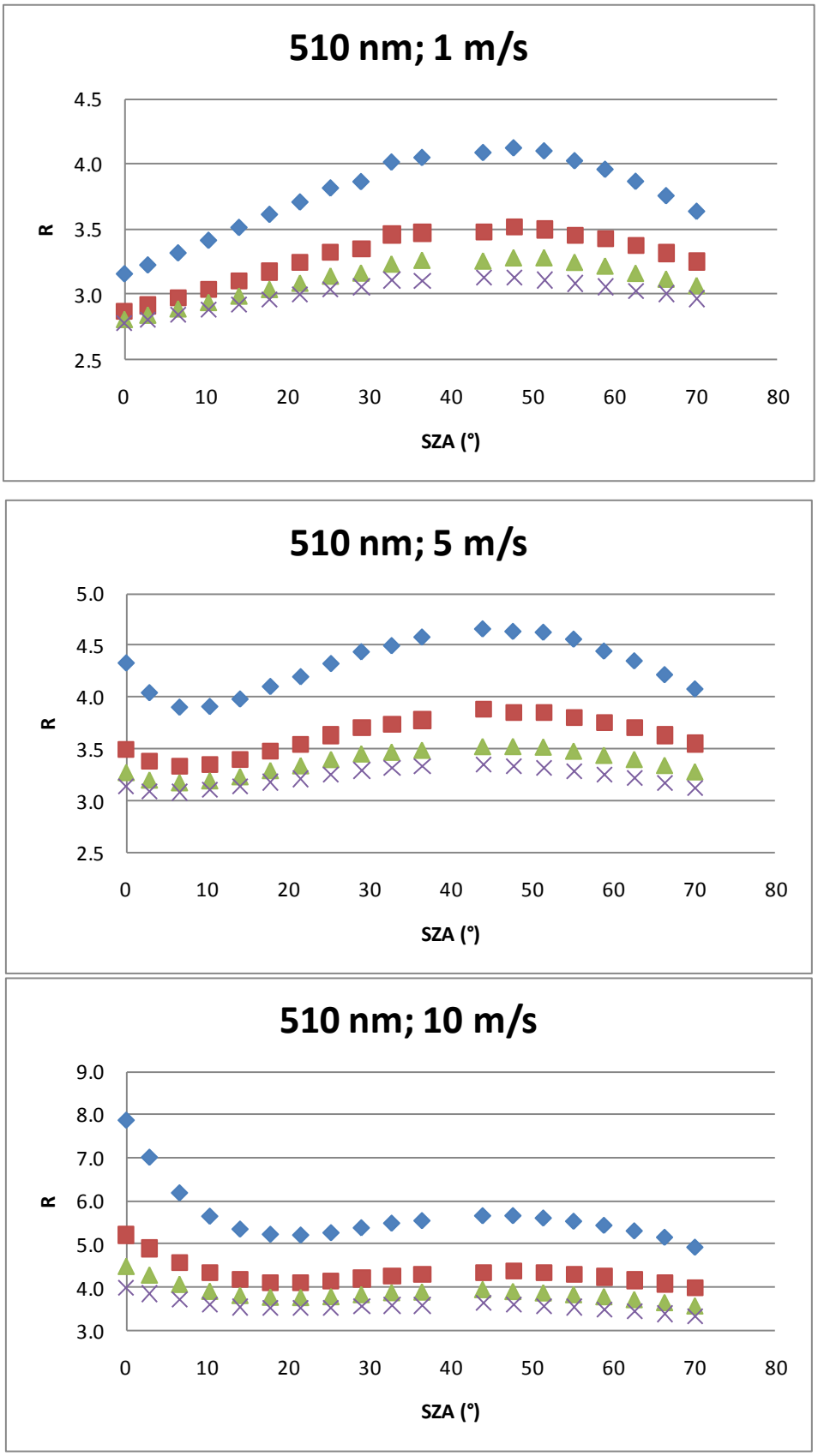

Figure 15: Reflection coefficient at 520 nm versus the solar zenith angle. The aerosol model is the model 3. Rayleigh (blue diamond), M4 with an AOT at 550 nm of 0.3 (red square), 0.6 (green triangle) and 0.9 (blue cross)

The spectral dependence of R is reported in figure 16.at two solar angles for te aerosol model M3 and an AOT at 550 nm of 0.3. The aerosol model corresponds to a standard for coastal areas. A small spectral dependence exists.

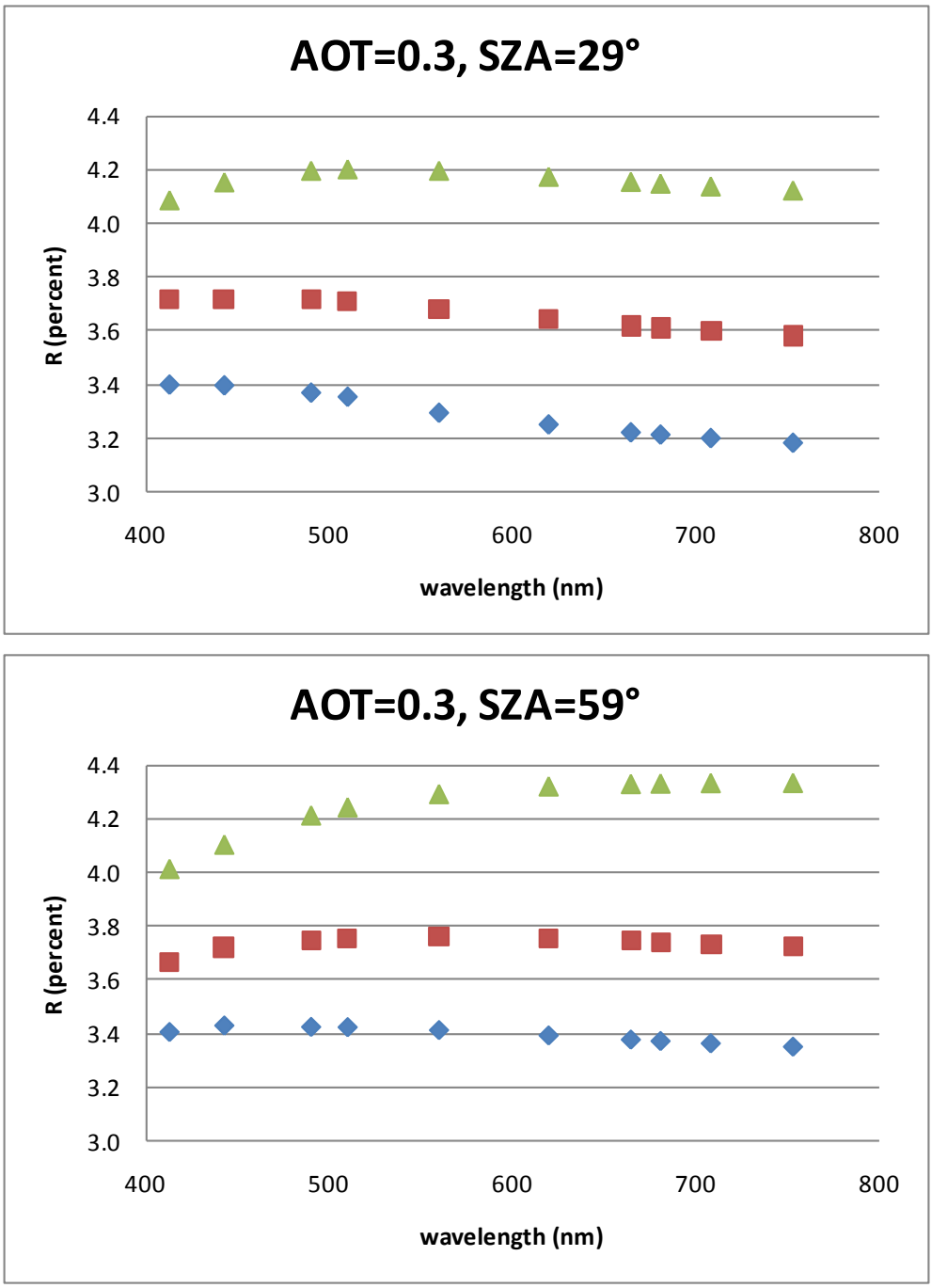

Figure 16: M3 with AOT=0.3 at 550 nm: Spectral dependence of the reflection coefficient at 2 SZA for three wind speeds: 1 m/s (blue diamond), 5 m/s (red square) and 10 m/s (green triangle)

The bias on the water reflectance is:

$$d\rho_w = \frac{(R_{SOS} - R) I_{down}}{\mu_s T(\vartheta_s)} \qquad (20)$$

Figures 17 to 19 give examples. If R_{sos} does not vary much in wavelength, the error is amplified at short wavelength both by the increase of the sky radiance and the decrease of the transmittance. The results are quite consistent with the specular case. The Rayleigh scattering is the major cause but the polarisation of the aerosols slightly amplifies the effect.

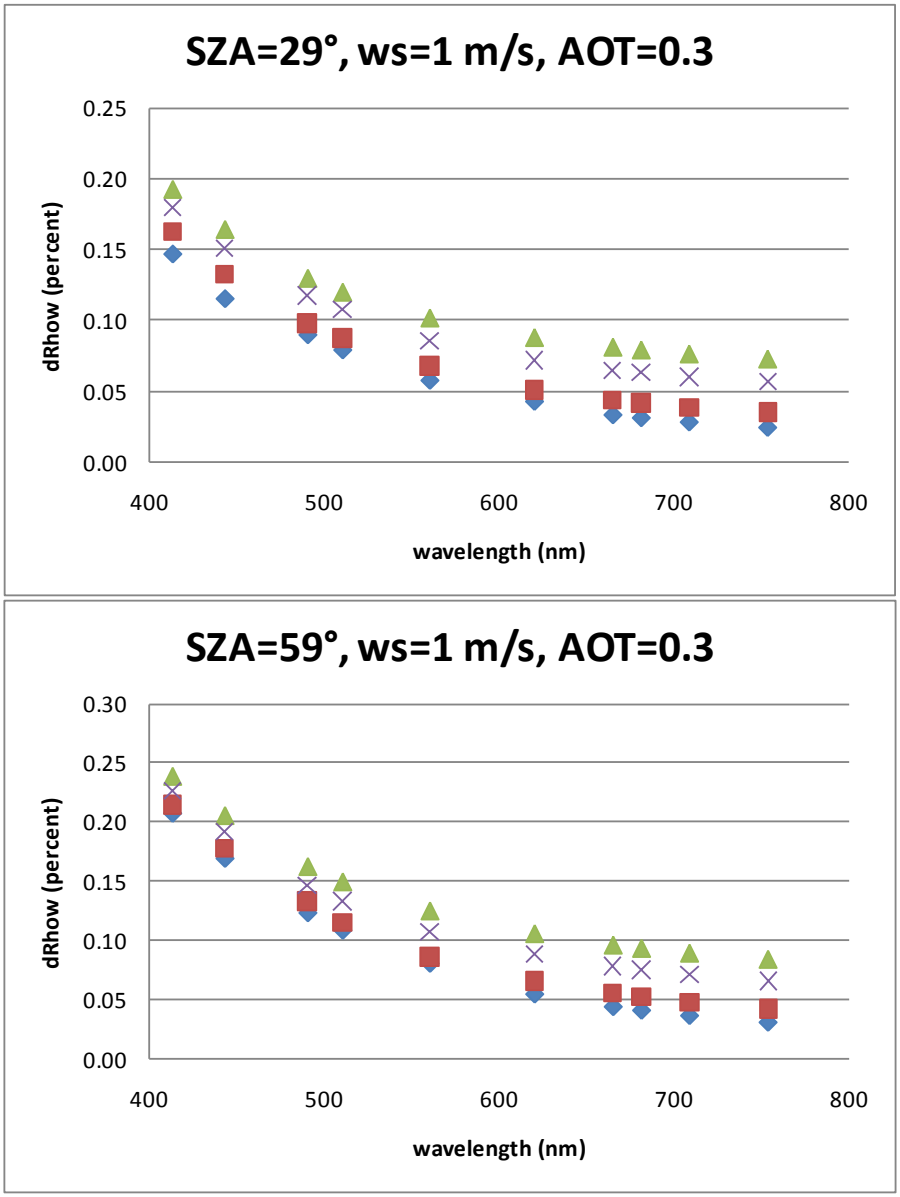

Figure 17: Wind speed of 1 m/s. Absolute bias on the water reflectance for two solar zenith angles versus the wavelength: The AOT at 550 nm is 0.3 for M1 (blue diamond), M2 (red square), M3 (blue cross) and 0.9 (green triangle).

The error increases with the wind speed. The Fresnel matrix is convoluted by the wave slope distribution, The terms of the Fresnel matrix increase with the incident angle. At high wind speed, more wave facets reflect the polarized light at larger incidence angles.

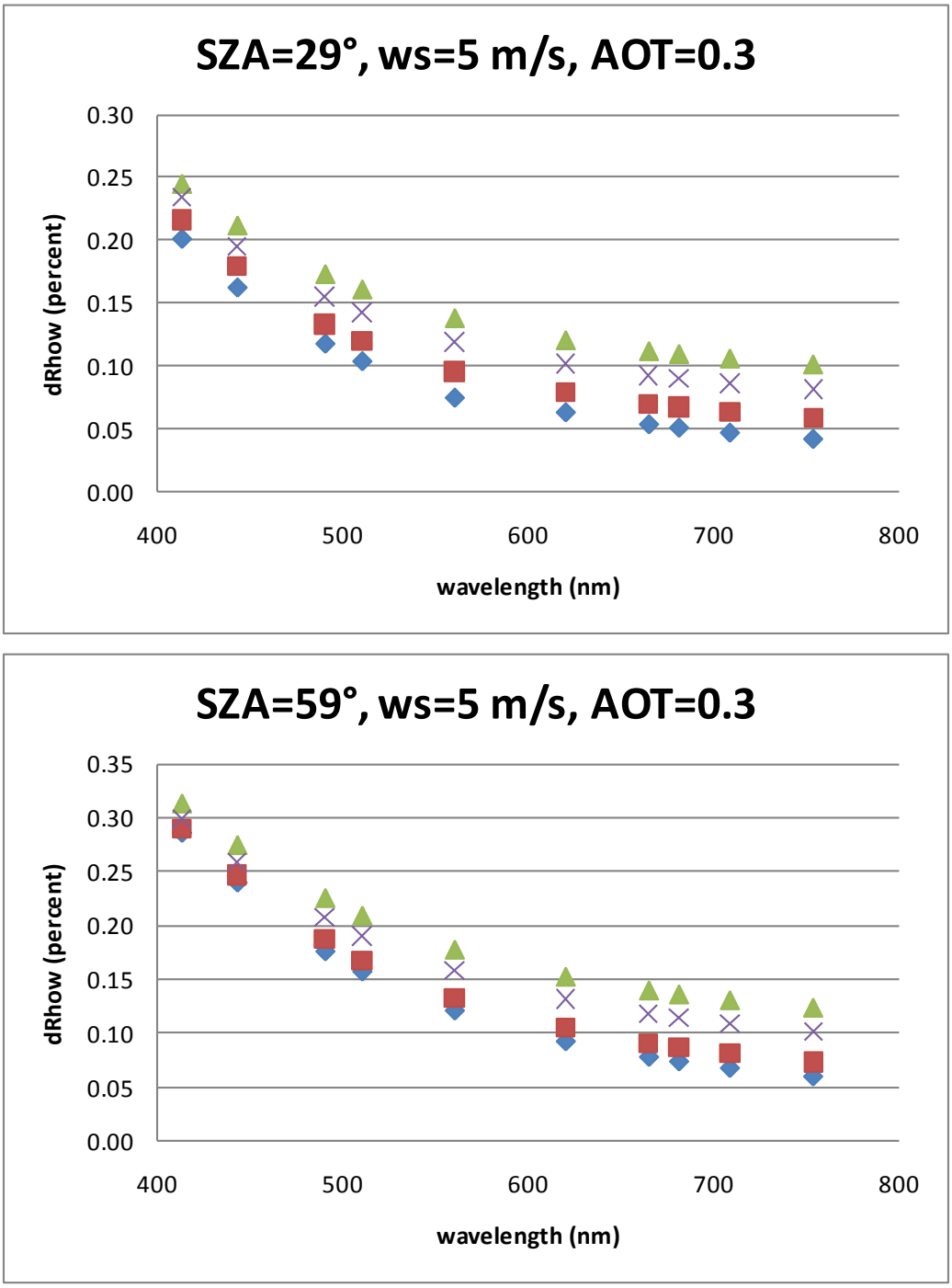

Figure 18: Wind speed of 5 m/s. Absolute bias on the water reflectance for two solar zenith angles versus the wavelength: The AOT at 550 nm is for M1 (blue diamond), M2 (red square), M3 (blue cross) and 0.9 (green triangle).

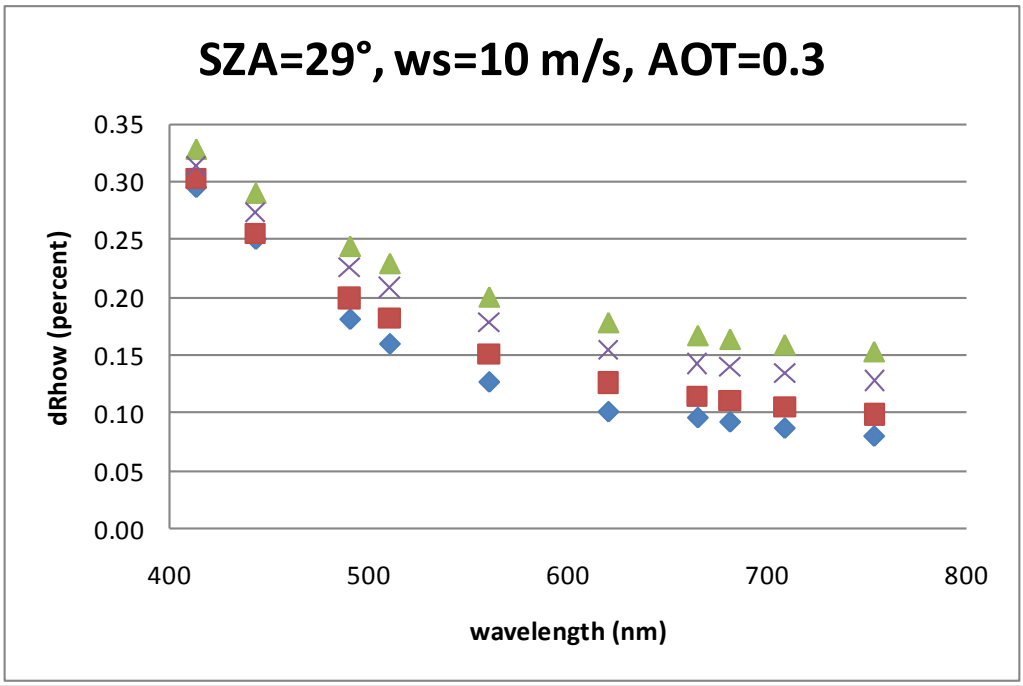

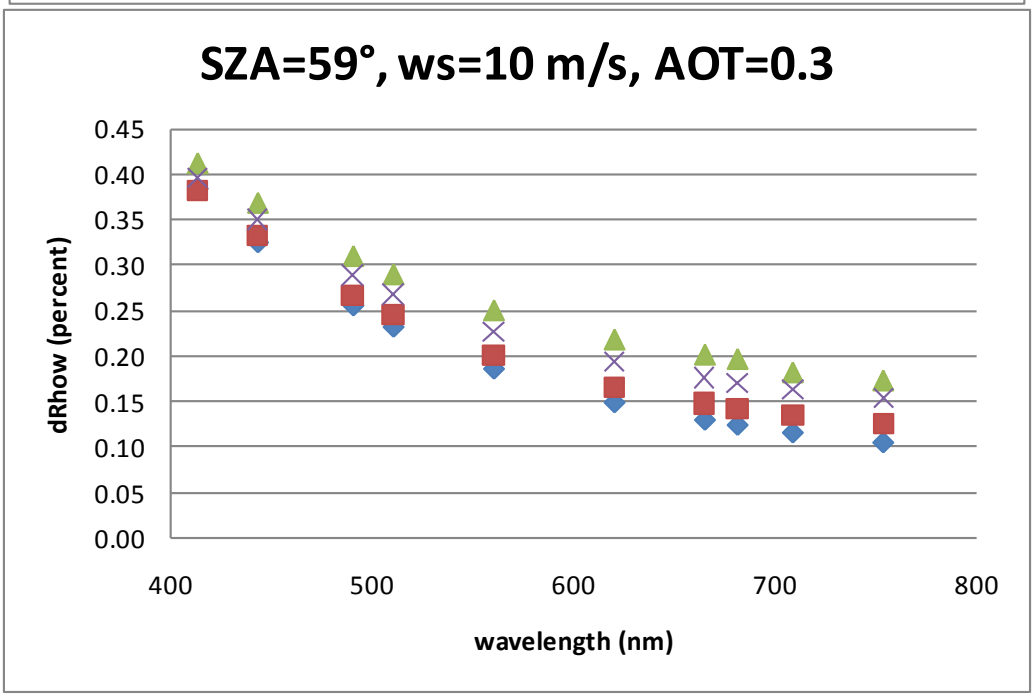

Figure 19: Wind speed of 10 m/s. Absolute bias on the water reflectance for two solar zenith angles versus the wavelength: The AOT at 550 nm is for M1 (blue diamond), M2 (red square), M3 (blue cross) and 0.9 (green triangle).

4) The polarisation of the aerosols

The above four aerosol models corresponded to a refractive index m=1.44. The polarisation is sensitive to m. Therefore, in order to study the influence of the aerosol polarization, we always selected the 4 power laws for

the size distribution, but we added two refractive indices (1.33 and 1.55). The influence of the refractive index, figure 20, appears comparable to the effect of the size.

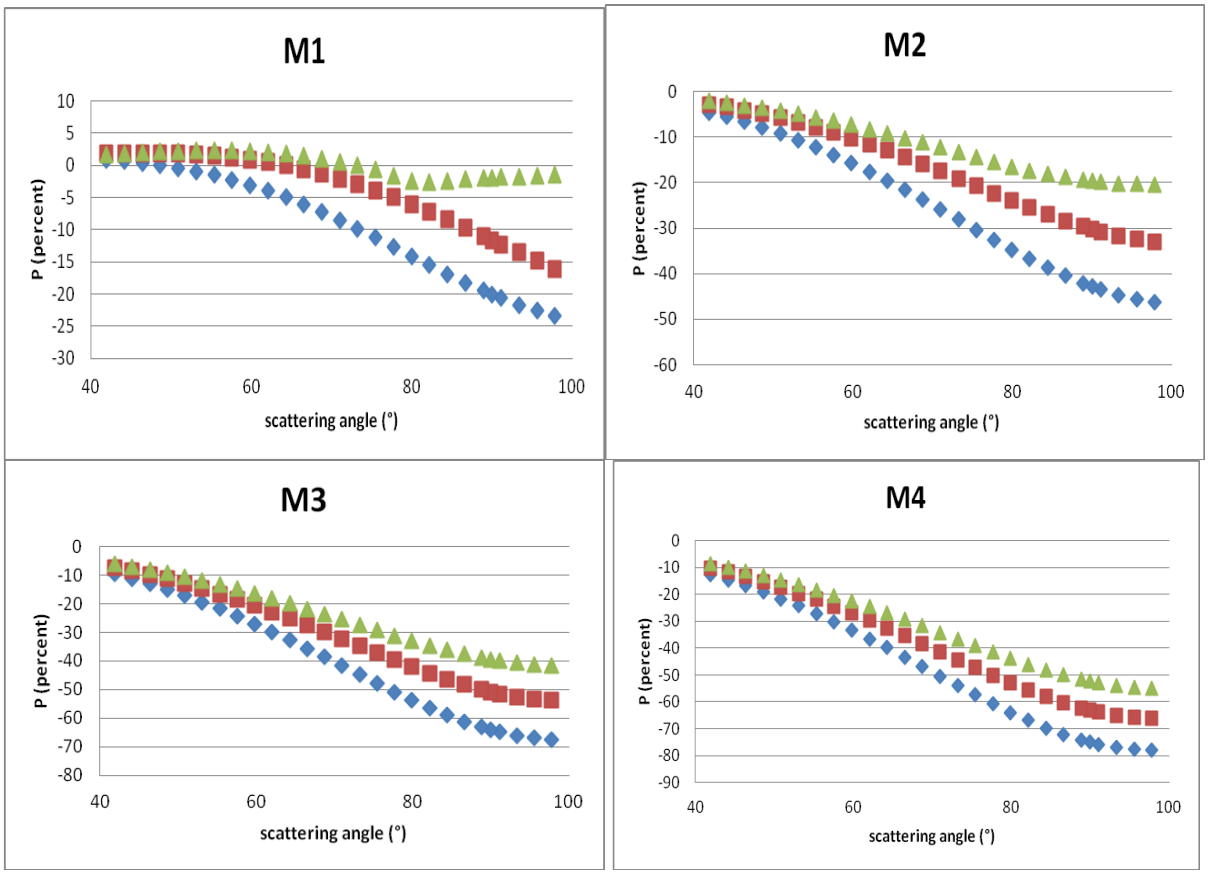

Figure 20: Polarisation ratio for the 4 size distributions (M1 to M4) and the 3 refractive indices: m=1.33 (diamonds), m=1.44 (squares), m=1.55(triangles)

We reported in figure 21 the reflection coefficients in B9, in the NIR to better see the impact of the aerosols

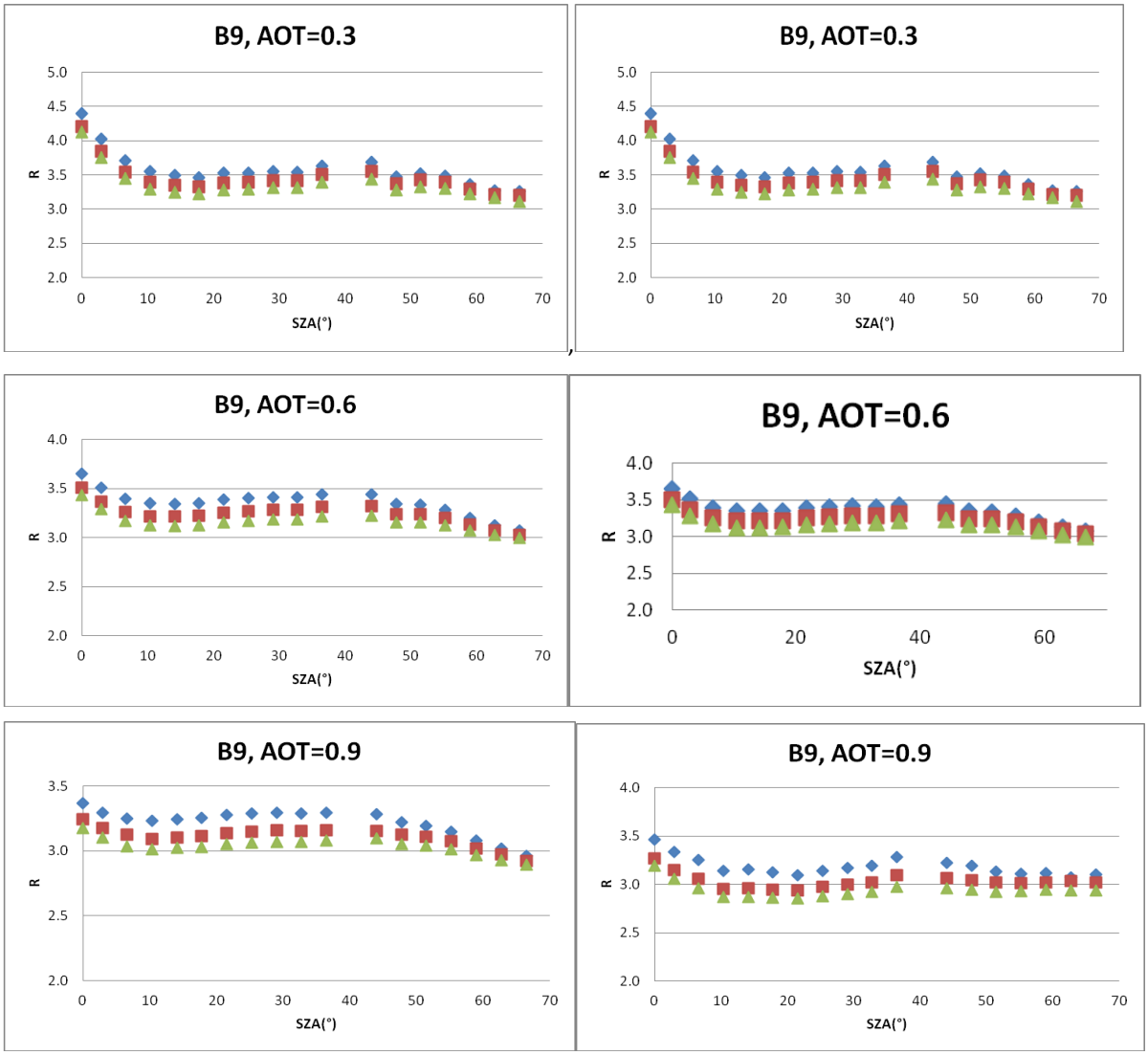

Reflection coefficient for M1 for the 3 refractive indices at 745 nm: 1.33 (blue diamond), 1.44 (red square) and 1.55 (green triangle)

The error, or the sensitivity to the refractive index, in reflectance is given as followed:

$$d\rho_w = \frac{(R_m - R_{1.44})I_{down}}{\mu_s T_{1.44}(\vartheta_s)} \qquad (21)$$

Because the polarisation increases when the refractive index decreases, positive values correspond to the pairs (1.33-1.44)and (1.44-1.55). Because the polarisation of the M4 aerosol model is the strongest, we reported in figure 21 the results in B2 and B9. When comparing to figure 13, the accurate knowledge of the polarization of the aerosols is a second order term. The first order term is the introduction of the polarisation of the Rayleigh.

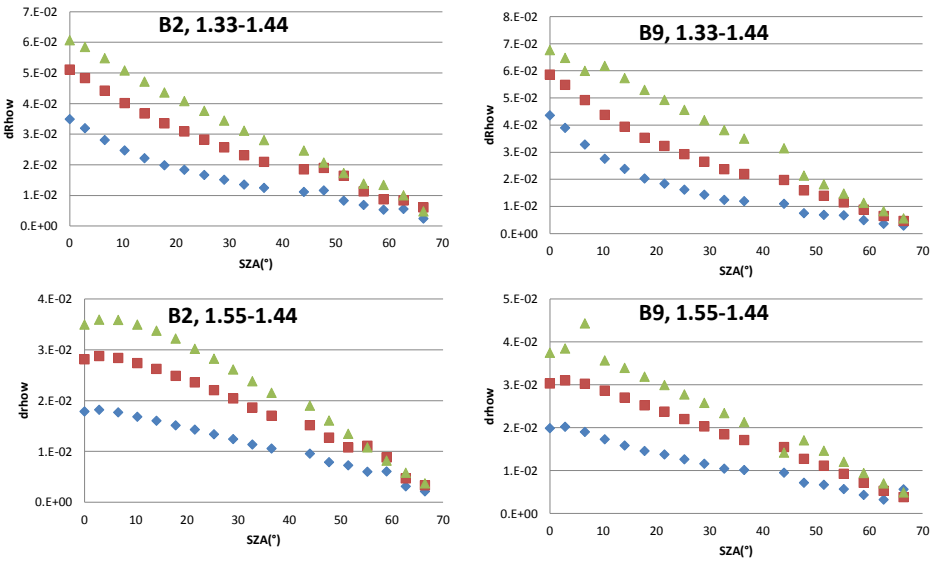

AOT=0.3 (blue diamond); 0.6 (red square); 0.9 (green triangles)

Figure 21: Impact on the water reflectance of the refractive index

4) Conclusion and recommendation

Yes, the total intensity (radiance) is affected by the polarisation state of the sky light; at least when the Fresnel reflection is highly polarized. In the blue, the Rayleigh scattering is the major cause associated to it high polarization. The effect is less important in the red first because the scattering is reduced. Small aerosols can highly polarised but in the same time, the AOT decrease is noticeable at larger wavelengths.

If there is a role of the polarisation of the aerosols, we need to know t his polarisation. The knowledge of the aerosol polarisation results from Mie computations with as input the micro physical properties of the aerosols. For small aerosols, we trend towards the Rayleigh-Gauss regime with as key parameter $(m-1)r/\lambda$. The smaller the refractive index m is, and the larger the polarisation is. A sensitivity driven by m suggests that an error on the knowledge of the aerosol polarisation as a small impact on the sky dome correction. Nevertheless, it is recommended to experimentally validate the aerosol polarisation. Some of the CIMEL instruments are equipped for polarisation measurements and can be used.

At the end, we need to include the polarisation in the correction of sky dome reflection. WP2 will address the correction of the Seaprism instrument while WP3 will cover the TRIOS.

We selected the TRIOS geometry at MUMM to conduct this study. The simulator can be used to generalized this study to other geometries (TRIOS at VZA=15°, 55° at any azimuth) and to other sensors Seaprism,...). In terms of VZA, small VZA reduces the polarisation of the Fresnel reflection but at low SZA, a sunglint contamination is possible. Conversely, high VZA will cancel the sunglint contamination at any SZA but increase the Fresnel polarisation.

If we need the polarisation of the sky light, then we can measure it. Already, some radiometers exist equipped to measure it. They can be used in a dual mode: sky and water. The Fresnel coefficients R1, R2 and R3 are given

above from the specular case. They can be convoluted by a wave slope distribution model in order to obtain a set of reflection coefficient associated to a wind speed.

References

COX, C., and W. MUNK, 1954. "Measurements of roughness of the sea surface from photographs of the sun glitter", *Journal of Optical Society in America*, 44 (11), pp. 838-888.

DEUZÉ, J.L., M. HERMAN, and R. SANTER, 1989. "Fourier series expansion of the transfer equation in the atmosphere-ocean system", *Journal of Quantitative Spectroscopy and Radiative Transfer*, 41 (6), pp. 483-494.

GORDON, H.R., and M. WANG, 1994. "Retrieval of water-leaving radiances and aerosol optical thickness over the oceans with SeaWiFS: A preliminary algorithm", *Applied Optics*, 33 (3), pp. 443-452.

Ruddick K., De Cauwer, V Young-Je Park and Moore G., 2006, Seaborne measurements of near infrared water-leaving reflectance: The similarity spectrum for turbid waters.Limnol. Oceanogr., 51(2), 2006, 1167–1179